PHY64 Lab 5

Toki Nishikawa, Hannah Magoon

May 13th, 2023

Contents

1 Background

In this experiment, Na22 sample is used as a positron source. The positrons are emitted with decay mechanism:

$$_{11}Na^{22} \longrightarrow_{10} Na^{22} + e^{+} + \nu_e \tag{1}$$

Decay of the Ne^{22} nucleus results in the emission of a 1.274MeV gamma ray.

This positron source is surrounded in a layer of plastic thick enough to stop most of the emitted positrons, but thin enough that the gamma rays resulting from annihilation of mechanism $e^{+} + e^{-} \longrightarrow \gamma + \gamma$ are allowed to escape. From this equation, we can see that if the annihilation occurs when the positron is at rest, then the energy of each gamma ray will be equal to the rest mass energy of an electron.

These emitted gamma rays are detected using two NaI crystals fixed to arms of a movable spectrometer. The spectrometer arems are initially set up on each side of the source so that they are directly opposite one another. Over the course of the experiment, the movable arm of the spectrometer is displaced by angles of up to $\pm 5°$. The rate of coincident gamma ray detection is measured as a function of spectrometer angle.

1.1 Experimental Setup

A diagram of the spectrometer setup is included below. It is important to note that the lead collimators used on each end of the spectrometerr have distinct geomtries. The moving spectrometer has a large aperature of 1.75", and the fixed spectrometer has a small aperature of 0.6". Lengths of the two lever arms were measured in the lab. Due to limitations of measuring tools available for use in the lab, these lengths were determined using piecewise measurements. To find uncertainty on the total lengths, we add the uncertainties of each measurement. This is because in the case of maximum possible error, each of our measurements will be off by the maximum possible uncertainty (in the same direction). The error in the total length measurement will be equal to the sum of the uncertainty values. The measured values and their uncertainties are provided later in the report.

We expect gammma rays from this setup to be produced in pairs. Our goal in this lab is to sense one gamma ray in each detector. To ensure that the gamma rays we are detecting result from this pairwise production, we use a coincidence setup. We set the first detector (Osprey1), to trigger a voltage pulse each time it detects a gamma ray within a specified energy range. This trigger prompts the second detector (Osprey2) to save the data it collected within a window of time surrounding the release of the trigger.

1.2 Determining ROI of Osprey2

To reduce the effects of false coincidences, we restrict the trigger window on Osprey1. Since we are only interested in 0.511 MeV gammas, we examine our calibration data and select a range of bin numbers centered on this peak. Events that fall within this range will trigger readout of Osprey1, and events outside of this range will be ignored. From visual inspection, we determined that the bin range [260,331] to be adequate. This range choice is displayed in the plot below:

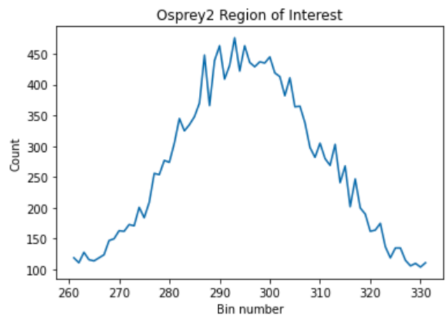

Figure 1: Visually selected 0.511MeV peak, Osprey2

With this setup, we collected 5 minute long acquisitions from Osprey1 for a variety of different angular displacements. Here, 0° refers to the position where Osprey1 and Osprey2 are positioned perfectly opposite one another. In the following sections, we describe an analysis method for this data that enables us to compare coincidence rates for each of these positions.

1.3 Determining ROI of Osprey1 Data

We were required to visually identify a Region of Interest (ROI) of the stationary detector (Osprey2) while in the lab. Events within this region generated a trigger signal sent to the movable detector (Osprey2). Since the peaks in the data were quite large and distinct from their surroundings, this was an adequate method of setting a ROI. However, when fitting the data from the second detector (OSprey1), we had the advantage of time and online analysis tools. Consequently, we implemented a more rigorous method. To define a region of interest, we examined the Osprey1 data taken at an angle of 0°. We fit the data to a Gaussian curve. We set our ROI to fall within the 2 sigma range of this Gaussian fit. From the fit, we find 2 sigma to be equal to 21.75549918 bins. We allow this range to set the ROI for all Osprey1 detector data. A plot of the fit is shown below:

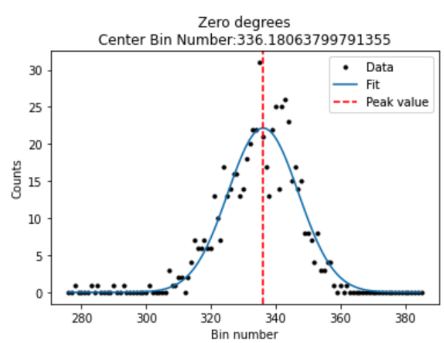

Figure 2: Gaussian fit to 0 degrees detector position

2 Analysis #1: Comparing coincidence rates

Next, we used a python function to sum the contents of each bin within the established ROI. A plot of the total counts as a function of detector angle is shown below:

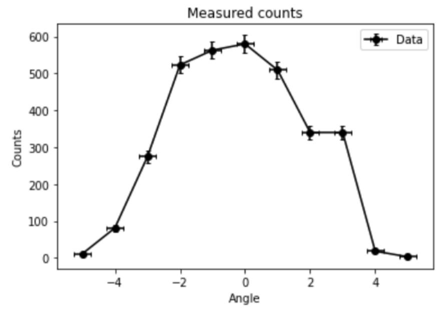

Figure 3: Measured data with sqrt(N) uncertainty

The uncertainty in the y-direction of each measurement is set equal to $\sqrt{N_{events}}$. This uncertainty approximation was suggested in the lab handout, to be used for random events of count N. The uncertainty in the x-direction is equal to 0.25 degrees, and was approximated by Toki in the lab as he moved the spectrometer. For the sake of consistency, Toki handled all adjustments to the spectrometer throughout the duration of the lab.

We note that we are plotting the counts seen by the detector, and not the count rate. This is acceptable because the acquisitions shown have identical time durations.

As a sanity check of our data-quality, we fit it to a gaussian distribution. As with Lab 4, an Orthogonal Distance Regression was used to account for uncertainty in both the recorded x and y values of our dataset. The results of this fit are included below. From this, we find that the center angle is -0.179. This value is not of particular use to the analysis, but it is helpful to benchmark our accuracy in setting up the detector

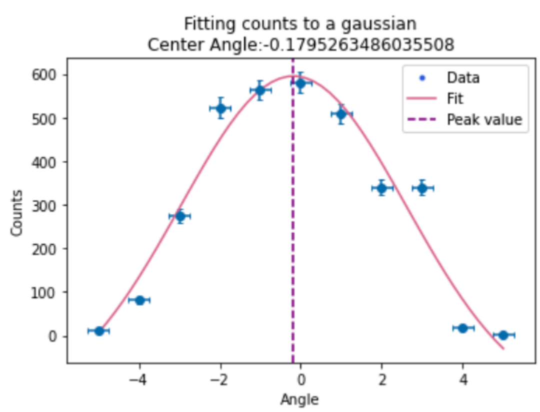

Figure 4: Finding center of dataset by fitting to a gaussian distribution

2.1 Detector geometry

In this section, we will use the geometry of the lab setup to determine the expected counts as a function of angle. A 2D sketch of the detector setup is included below.

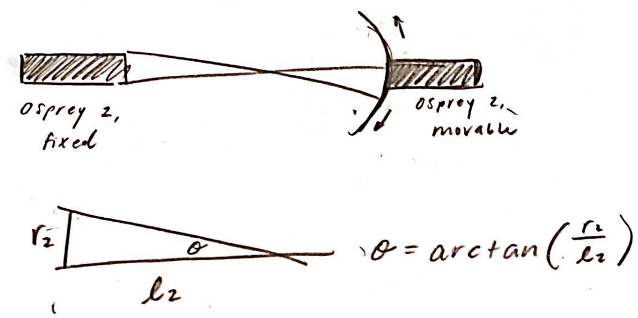

Figure 5: Stationary detector geometry

Here, we see that the stationary detector carves out a conical region of coincidence. Gamma rays emitted from the source within this sector will successfully enter the aperture of the stationary detector. We can use properties of the detector geometry to determine the angle that defines this conical sector:

$$\theta = arctan(\frac{r_2}{\ell_2}) \tag{2}$$

Where here, r_2 refers to the radius of Osprey2, and ℓ_2 refers to the distance between Osprey2 and the center of the source. This distance was found using the sum of three measurements. The measurements and their uncertainties are included in here:

Location	**Variable**	**Measurement**	**Uncertainty**
Sample ⟶ collimator	n/a	13.9 cm	± 4 mm
Collimator ⟶ aperture	n/a	10.1cm	± 1 mm
TOTAL LENGTH	ℓ_2	24.0 cm	± 5 mm
DIAMETER	$2 \cdot r_2$	1.2 cm	± 1 mm

Figure 6: Measurement of length to stationary spectrometer arm

Plugging these values into the equation above, we find:

$$\theta = arctan(\frac{\frac{1}{2}1.2cm}{24cm}) \tag{3}$$

$$\theta = 1.432^\circ \tag{4}$$

The path of gamma rays incident on the Osprey2 sweeps out a conic sector with angle $\theta = \pm 1.432^\circ$ on each side of the origin. Next, we look at the geometry of Osprey1. We look for the range of placements in which it can detect gammas traveling at angles of up to $\pm\theta$ about the 180° mark. Note that Osprey 2 will be able to detect gammas from this This is because the detector has a nonzero radius. There will be some angles larger than θ at which some portion of the detectors aperture intersects the conic sector. A diagram of this geometry is shown below:

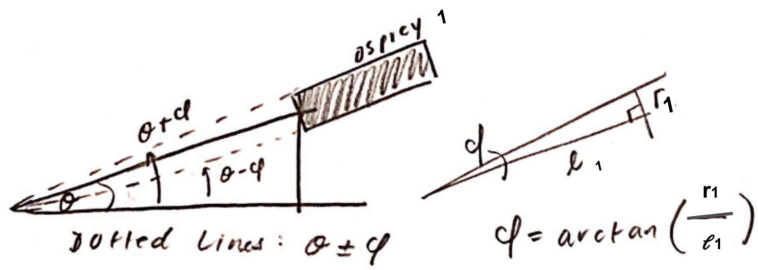

Figure 7: Movable detector geometry

Next, we project the conic sector to the other side of the source. Within this sector, straight lines can be drawn through the source to the stationary detector. We use the geometry of Osprey1 to determine the angular location where part of its aperture intersects this sector. As shown in the sketch, for angles less than $\theta - \varphi$, the entirety of Osprey1's aperture is contained within the sector. This will result in the highest possible coincidence rates. When Osprey1 is located between angles $\theta - \varphi$ and $\theta + \varphi$, its aperture partially intersects the sector. And finally, when it is placed at an angle $> \theta + \varphi$ on either side of the origin, the detector should not receive any coincident gamma rays. To find the parameter ϕ, we use the geometric relation:

$$\varphi = arctan(\frac{r_1}{\ell_1}) \tag{5}$$

This equation comes from the above drawing; since Osprey1 sits on a rotating spectrometer arm, we know that at its center, its aperture is perpendicular to the length ℓ to the source. To solve this equation, we use our measurements of r and ℓ. The length ℓ_1 in question was found using:

Location	Measurement	Variable	Uncertainty
Sample $\longrightarrow$ aperture	ℓ_1	44.5 cm	$\pm$ 4 mm
Diameter	$2 \cdot r_1$	4.6 cm	$\pm$ 1 mm

Figure 8: Measurement of length to movable spectrometer arm

We substitute these values to find φ:

$$\varphi = arctan(\frac{\frac{1}{2}4.6cm}{44.5cm}) \tag{6}$$

$$\varphi = 2.9587° \tag{7}$$

2.2 Modeling the coincidence rate

Given this information, we expect to see some response for detector angles within range $[-(\theta + \varphi), \theta + \varphi] = [-4.5°, 4.5°]$. As the detector angle moves away from the central 0° mark, we expect to see count rate that falls off. To predict the how this rate falls off, we need to first model the rate at which Osprey1's aperture exits the coincidence region. We know that the rate of events seen by Osprey1 will be related to the area of its aperture that lies within this coincidence region. Expressing this quantity as a function of the detector angle is quite difficult, and I struggled to write an analytical expression for it. After hours of geometric confusion, I decided to take advantage of the fact that our data-set is discrete. I used NX CAD simulation software to model this setup, and used the software to calculate the area of the aperture that intersects the conical coincidence region. I repeated this procedure for all angles in the set. Images of this setup are shown below. Here, the purple cone represents the events that can be seen by Osprey2. The colorful disks represent the aperture of Osprey 2. We use the software to identify the 2D area of intersection between these two elements.

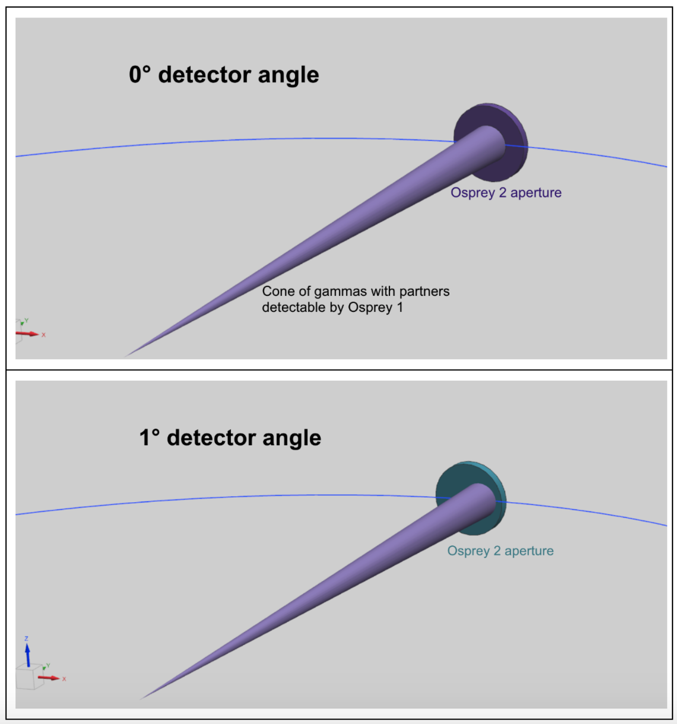

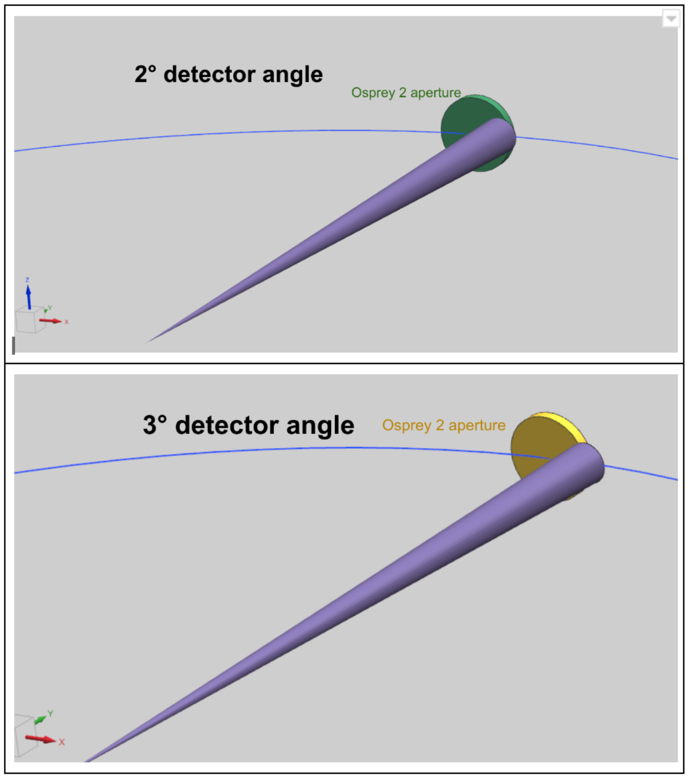
2° detector angle
Osprey 2 aperture
3° detector angle
Osprey 2 aperture

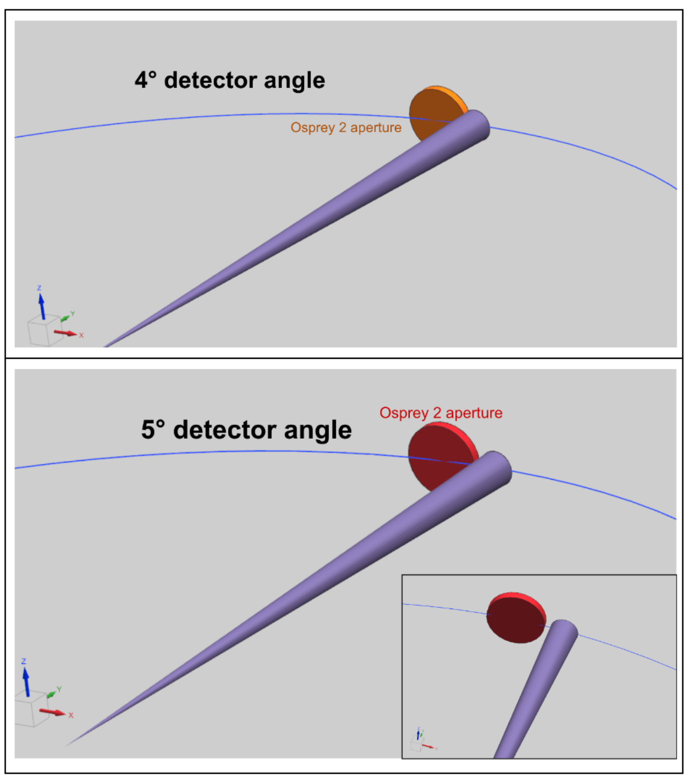
4° detector angle
Osprey 2 aperture
5° detector angle
Osprey 2 aperture

The fraction of the coincidence cone contained within Osprey 1's aperture is displayed in the follow plot:

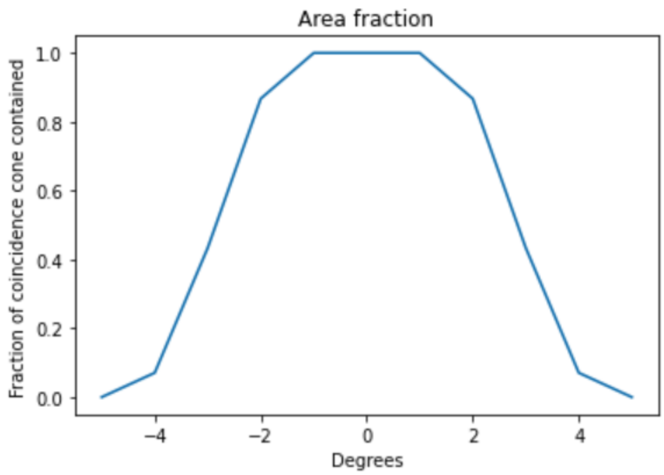

Next we convert this plot into a model for prediction for coincidence rates. To do this, we multiply the area fraction (plotted above) by the maximum measured coincidence rate. This rate is measured at the 0° detector position, and serves as a scale factor. To predict coincidence rates across the remaining detector positions, we multiply the maximum coincidence rate by the fraction of the 2D coincidence region contained by the detector's aperture in the new location. A plot of the expected coincidence rates is shown below:

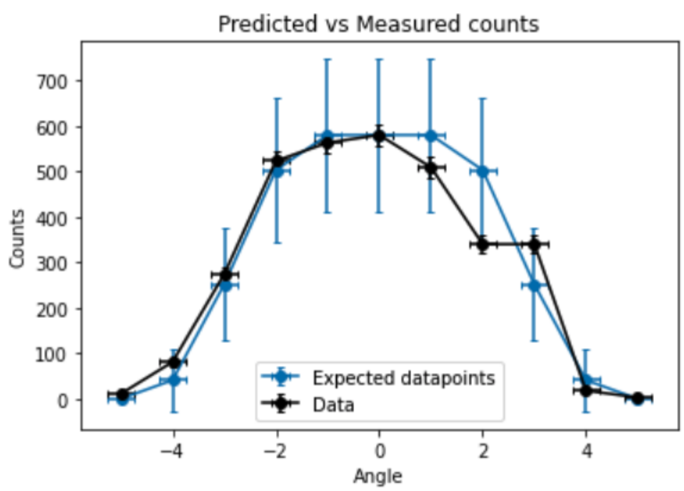

We have two sources of uncertainty in our expected coincidence rates. First, the uncertainty in the number of counts is given by $\sqrt(N)$. Our scale factor (the maxium observed coincidence rate) also has uncertainty $\sqrt(N)$. The equation used for our predicted values is:

$$(\text{area fraction}) \times (\text{max counts}) \tag{8}$$

The uncertainty is therefore given by:

$$\sigma(\text{counts}) = \sqrt{(\text{area fraction} \times \sigma(n_{max})^2 + (n_{max} \times \sigma(\text{area fraction}))^2} \tag{9}$$

Also on this plot is the actual data we collected in-lab. We used python to get the number of data-counts within the detector ROI for each of our datasets. Following the direction in the lab manual, we assigned each of these counts an uncertainty value of $\sqrt{N}$. This falls from the assumption that our data fits a gaussian distribution. As shown below, this assumption begins to break down at high detector angles. This is due to the low number of counts. Regardless, we used the $\sqrt{N}$ uncertainty for all datapoints because it is expected to hold true for datasets with counts $N > 20$.

We find our model to be in very good agreement with the data. We note that each datapoint falls within the region of uncertainty of our predictions. When comparing the two datasets, we find a mean squared error of 62.4423773. This value is small compared to the number of counts examined in the dataset.

Given this information, we conclude that our data is consistent with the assumption that the electrons and positrons are initially at rest. Our predicted model of the fall-off rate is well-aligned with the data. There is quite a bit of uncertainty in both our model and the data, however, and it may be possible to get better agreement within the uncertainty ranges if we accounted for non-zero initial electron/positron positions. Another way to improve this prediction would be to assume that the NaI crystal is not a point-like source.

3 Analysis #2: Background Rates

To find background rates, we position Osprey 2 at an angle of 20°, which is located fully outside the region of coincidence. Next, we find background rates for each detector, and compare these rates to the false coincidence rate.

3.1 Background Rate of Osprey 1

We first find the number of events by summing the contents of the bins within the region of interest, and we assume $\sqrt{N}$ uncertainty on this value. For Osprey 1, we identify 10291 ± 101.444 counts. To convert this to a background rate, we divide by the time interval of the acquisition. This acquisition time was measured using the lab computer and its uncertainty will be negligible. From this, we find a rate of 8.5758 counts/second. From the propagation of uncertainty formula, the uncertainty in the background rate will equal $\frac{1}{t}\sigma_{counts}$. Our uncertainty is therefore ± 0.084536. Compiling this information:

$$n_1 = 8.5758 \pm 0.084536 \tag{10}$$

3.2 Background Rate of Osprey 2

Once again, we find the number of events by summing the contents of the bins within the region of interest, and we assume $\sqrt{N}$ uncertainty on this value. For Osprey 2, we identify 18929 ± 137.583 counts. To convert this to a background rate, we divide by the time interval of the acquisition. From this, we find a counts per second rate of:

$$n_2 = 5.5716 \pm 0.040496 \tag{11}$$

3.3 False Coincidence Rate

The false coincidence rate is given by the product of these two rates. We an coincidence sync of time τ, we expect a rate of $n_1 n_2 \tau$ fake coincidences. The lab manual gives a sync signal duration of 250ns. Plugging in our values from earlier, we find:

$$n_1 n_2 \tau \pm \sqrt{(n_2 \tau \sigma_{n_1})^2 + (n_1 \tau \sigma_{n_2})^2} \tag{12}$$

$$= 8.5758 \cdot 10^{-5} \pm 1.4629 \cdot 10^{-7} \tag{13}$$

To test the validity of this model, we took a 20 minute long coincidence measurement with the two detectors offset by an angle of 20°. Within the region of interest, only one event was detected:

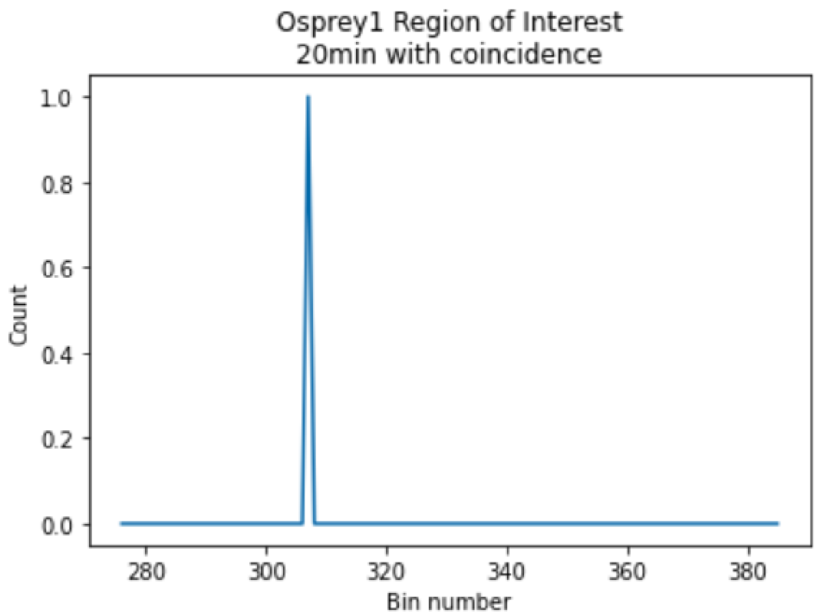

Figure 9: Background rate of coincidence detections

We assign error of $\sqrt{N} = \pm 1$ to this measurement. To convert this to a rate, we divide by the time interval of the acquisition and propagate the uncertainty using same method as before. This yields a coincidence per second rate of:

$$8.33333 \cdot 10^{-4} \pm 8.33333 \cdot 10^{-4} \tag{14}$$

The predicted and measured false coincidence rates fall within the uncertainty range of one another. Our background rate results are therefore consistent.

4 Analysis #3: Interpretation

With this information, we can transform the result from part #1 of the lab to a rate value with the backgrounds subtracted. Since the background rate is so low, this does not really impact the rates plotted. Nevertheless, this value is subtracted from all the rates in the dataset. A plot of this information is shown below.

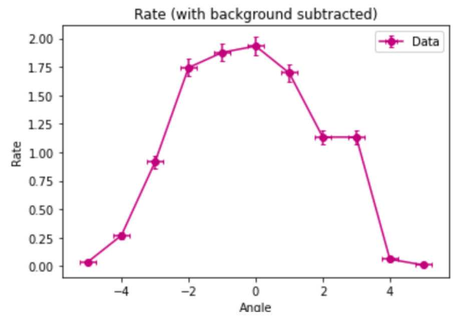

Figure 10: Detected rate as a function of angle

Since our background rate was negligible, this plot presents as simply a scaled version of the part from the first analysis section. We interpret its results (and the fit from before) to mean that the assumption that the position/electron system is initially close to rest is a valid assumption. The measured counts agree with our model. When the positron and electron annihilate, the energy of the gamma rays produced in the event is almost entirely equal to the rest mass energy of the two particles.